sustainability

MDPI

Article

Enhancing Mangrove Aboveground Biomass Estimation with UAV-LiDAR: A Novel Mutual Information-Based Feature Selection Approach

Shan Huang [1,2], Zhiwei Zhang [1,2,*], Yonggen Sun [2], Weilong Song [2] and Jianing Meng [1,2]

[1] College of Geodesy and Geomatics, Shandong University of Science and Technology, Qingdao 266590, China; hshan@fio.org.cn (S.H.); mengjianing@fio.org.cn (J.M.)
[2] Research Center of Coastal Science and Marine Planning, First Institute of Oceanography, MNR, Qingdao 266061, China; syg@fio.org.cn (Y.S.); songwl@fio.org.cn (W.S.)
* Correspondence: zzw@fio.org.cn

Abstract: It has been well observed that accurate estimation of the aboveground biomass (AGB) of mangrove forests is critical for evaluating ecosystem health, carbon sink capacity, and sustainable development. This study utilizes UAV-LiDAR data and field measurements to develop an AGB inversion model based on 26 feature variables. We employed three machine learning algorithms—random forest (RF), extreme gradient boosting (XGBoost), and support vector machine (SVM)—to estimate mangrove AGB in the Xinyingwan region of Lingao County, Hainan Province, China. The key findings include that: (1) the SVM algorithm demonstrated the highest predictive accuracy, with an R^2 of 0.8853 and RMSE of 0.4766 kg/m^2, making it most suitable for this study; (2) the proposed zero-importance feature selection method based on mutual information (MI) outperformed traditional techniques, selecting more effective variables for model development; (3) in the SVM model, variables selected using the zero-importance feature selection method based on MI yielded the best prediction accuracy; and (4) the estimated AGB in the study area ranged from 1.97 to 5.23 kg/m^2, with an average of 3.83 kg/m^2. This study not only provides valuable data for mangrove ecosystem conservation and restoration but also offers a scientific basis and technical framework for future biomass estimation and carbon stock assessments.

Keywords: mangrove forests; aboveground biomass; UAV-LiDAR data; mutual information; SVM algorithm

check for updates

Academic Editor: Tommaso Caloiero

Received: 10 January 2025
Revised: 6 March 2025
Accepted: 14 March 2025
Published: 28 March 2025

Citation: Huang, S.; Zhang, Z.; Sun, Y.; Song, W.; Meng, J. Enhancing Mangrove Aboveground Biomass Estimation with UAV-LiDAR: A Novel Mutual Information-Based Feature Selection Approach. *Sustainability* **2025**, *17*, 3004. https://doi.org/10.3390/su17073004

Copyright: © 2025 by the authors. Licensee MDPI, Basel, Switzerland. This article is an open access article distributed under the terms and conditions of the Creative Commons Attribution (CC BY) license (https://creativecommons.org/licenses/by/4.0/).

1. Introduction

Mangrove forests, crucial ecosystems in tropical and subtropical coastal areas, are extensively distributed in intertidal and marshy coastal zones [1]. These forests provide unique ecological values and essential environmental functions, playing a vital role in coastal stabilization, biodiversity protection, climate regulation, and the provision of a wide range of ecosystem services [2,3]. Moreover, mangrove forests serve as habitats for commercially significant fish species and endangered marine organisms [4,5]. In addition to their ecological importance, mangrove forests are a critical component of the marine "blue carbon" ecosystem, exhibiting remarkable carbon sink capacity [6,7]. Despite covering only 1% of global land area, mangrove forests account for approximately 5% of the world's total carbon sequestration, highlighting their significant role in mitigating climate change [8]. As a natural solution to climate change, mangroves efficiently absorb carbon dioxide

through photosynthesis and store carbon in plant biomass, detritus, and soil organic matter, contributing significantly to global carbon sequestration efforts, which emphasizes the importance of mangrove ecosystems in mitigating climate change and advancing sustainable coastal management [9–11].

On 20 September 2022, the Global Mangrove Alliance (GMA) published "The State of the World's Mangroves 2022" report [12], highlighting a global net loss of approximately 5245 square kilometers of mangrove forests since 1996. The primary direct drivers of this loss include aquaculture development (26.7%), followed by natural retreat contributing to 25.9%, alongside other unsustainable coastal development forms [13–15]. In response to this alarming trend, the Ministry of Natural Resources (MNR) and the State Forestry and Grassland Administration (SAGA) of China introduced the Special Action Plan for the Protection and Restoration of Mangrove Forests (2020–2025) in August 2020 [16]. This plan emphasizes comprehensive strategies for protection, restoration, and management alongside research on mangrove forest carbon sink projects. Furthermore, in October 2021, the State Council of China launched the Action Program for Carbon Peak by 2030, calling for the assessment of carbon sinks in oceans, forests, and other ecosystems and fostering marine carbon sinks [17]. Mangrove aboveground biomass (AGB), as a key component of carbon sinks, plays a pivotal role in conducting quantitative research and understanding the distribution patterns of carbon within mangrove ecosystems. Accurate AGB estimation provides significant theoretical support for assessing the health status and productivity of these ecosystems. Moreover, it holds substantial importance for the conservation, restoration, and management of mangroves, as well as for advancing our studies on the global carbon cycle and climate change.

Traditional methods of estimating mangrove biomass rely primarily on field measurements but encounter significant challenges due to the coastal intertidal distribution of mangroves, which makes manual surveys difficult and time-consuming. These methods also suffer from poor timeliness, low mapping accuracy, and can cause considerable damage to vegetation, leading to substantial errors in biomass estimation [18,19]. In contrast, remote sensing technologies offer distinct advantages over traditional field-based methods. Optical remote sensing, for example, enables simultaneous coverage of extensive mangrove areas, provides high temporal resolution, and is not constrained by geographic conditions, making it an efficient, accurate, and comprehensive tool for monitoring mangrove ecosystems [20,21]. Early forest biomass estimation efforts predominantly relied on low- to medium-resolution optical remote sensing data, such as MSS, TM, ETM+, and MODIS [22–25]. More recent studies have leveraged medium-resolution optical remote sensing data from platforms such as Sentinel-2, Landsat, and SPOT, as well as high-resolution imagery from WorldView and QuickBird satellites, to estimate mangrove AGB, yielding promising inversion results [26–29]. However, passive remote sensing techniques, such as optical data, are often impeded by atmospheric conditions and cloud cover, and their limited ability to penetrate the forest canopy significantly hinders the acquisition of detailed information about the vegetation structure beneath the canopy [30]. In contrast, active remote sensing techniques, such as light detection and ranging (LiDAR) and synthetic aperture radar (SAR), utilize actively emitted electromagnetic waves or lasers to gather ground-based information. These techniques can effectively penetrate vegetation layers and provide detailed vertical structural data, which are crucial for accurate mangrove AGB estimation [31]. While SAR data expand the range of available remote sensing information, its practical use is constrained by several factors, such as complex interpretation, resolution constraints, surface property influences, polarization and band selection limitations, and high costs when compared with LiDAR data. Nonetheless, LiDAR offers superior capabili-

ties in terms of providing high-resolution, precise, and reliable data for mangrove biomass estimation [19,20].

Unmanned aerial vehicle-LiDAR (UAV-LiDAR), as an emerging and rapidly evolving active remote sensing technology, has significantly enhanced the research and application in the field of remote sensing in recent years. It is widely used in key areas such as environmental monitoring, topographic mapping, and forest resource surveys. Airborne LiDAR technology effectively penetrates the canopy layer, capturing precise data from the top vegetation to the ground at various levels. Compared with optical imagery and SAR data, LiDAR technology not only demonstrates higher accuracy and reliability but also offers all-weather operational capability and rapid data acquisition features, making it a powerful tool for mangrove monitoring [32–34]. Recent studies have demonstrated the effectiveness of UAV-LiDAR for estimating mangrove AGB. For instance, Ref. [35] used UAV imagery and LiDAR point cloud data to estimate the AGB of single-timber species in Qi'ao Island Mangrove Nature Reserve in Zhuhai City, Guangdong Province. A tree height-breast diameter regression model was developed based on ground-based LiDAR data, and an optimized tree height-based anisotropic growth equation was applied to estimate AGB at the individual tree level. In another study [36], UAV multispectral remote sensing data and airborne LiDAR point cloud data were used to identify mangrove species in the Maowei Sea Mangrove Reserve in Guangxi. By combining these data with measured mangrove growth parameters, a regression model was constructed to estimate AGB in the study area. Ref. [37] used LiDAR data to quantify mangrove vegetation height in Darwin Harbour, northern Australia, and establish a relationship model that could be applied to remote areas, enabling mangrove AGB quantification. Moreover, Ref. [38] conducted a comparative study of different allometric growth equations to evaluate their effectiveness in estimating mangrove AGB, demonstrating the potential of LiDAR for accurate biomass and carbon stock estimation in mangroves. Despite these advances, the application of LiDAR's for mangrove biomass monitoring remains relatively underexplored, and further research is needed to fully realize its potential for large-scale mangrove monitoring and carbon stock estimation.

Models for estimating mangrove AGB are generally categorized into parametric and nonparametric models. Parametric models, including linear models and multiple regression models, are often used in biomass estimation. However, these models have limitations, such as a fixed structure that can be challenging to adapt to the varying growth characteristics of mangrove forests in different environments. Furthermore, they often fail to capture the complex nonlinear relationships typically found in such ecosystems. In cases with numerous independent variables, multiple regression models are prone to overfitting, reducing their generalization capability and predictive accuracy, which limits their application in AGB estimation [39,40]. With advancements in computer technology, nonparametric machine learning algorithms have emerged as more robust alternatives to traditional parametric models for estimating mangrove AGB. Compared with parametric models, nonparametric machine learning models, such as support vector machine (SVM), back-propagation neural network (BPNN), extreme gradient boosting (XGBoost), and random forest (RF), offer significant advantages in handling large-scale, multi-source remote sensing data. These nonparametric models excel at capturing complex nonlinear relationships and interactions among variables, leading to high prediction accuracy, particularly in cases involving large datasets with intricate relationships among variables. As a result, they have gained widespread use in biomass estimation for forests, grasslands, and other crops [41–44]. For example, Zhang [45] used the RF algorithm to estimate mangrove biomass in a study area, incorporating ground-truthed sample data and LiDAR point cloud data. The method demonstrated high fitting accuracy, as confirmed by the

validation against ground-truthed data; Luo [40] compared four gradient-boosted decision tree algorithms based on UAV-LiDAR data, ultimately selecting the XGBoost method due to its superior fitting performance to estimate the AGB of petal-less Morus alba in the Maowei Sea area of Beibu Bay. Additionally, Zhang [46] employed a watershed segmentation algorithm based on canopy height model (CHM) data to delineate single-tree canopy boundaries. By integrating LiDAR-derived variables and ground-measured data, they developed an AGB estimation model using RF and SVM, with both models showing high prediction accuracies; Tian [47] used eight different machine learning models based on variables such as canopy height, vegetation indices, texture indices, and LiDAR point cloud data from UAVs to estimate the AGB of mangrove forests of different species in the Beibu Gulf. The study found that XGBoost and RF models exhibited the highest estimation accuracies. Moreover, Jozdani [48] combined the texture features of optical images with ground-truth data to establish AGB estimation models using RF and SVM. A similar study in Daxinganling, China, used a combination of optical image texture features and airborne LiDAR data to compare various machine learning algorithms, including RF, bagging trees (BTs), gradient boosting trees (GBs), XGBoost, and SVM. The results indicated that the SVM model demonstrated the best performance in terms of both modeling effect and prediction accuracy. Although XGBoost, RF, and SVM models have demonstrated strong performance on high-dimensional data and excel at handling nonlinear relationships [49–51], their applicability to mangrove AGB estimation in different regions and the accuracy of these models in such contexts warrant further analysis and validation.

Feature selection is crucial in machine learning and statistical modeling as it reduces redundancy, simplifies model complexity, enhances prediction accuracy, and improves model generalization. However, many existing feature selection methods struggle to effectively handle complex nonlinear relationships, tend to overfit, and have limited interpretability. To address these challenges, this study focuses on the Xinyingwan area of Limgao County, Hainan Province, utilizing UAV-LiDAR data alongside ground-truth mangrove data. We proposed a novel feature selection approach based on mutual information, termed the zero-importance feature variable method. In this study, three machine learning algorithms—XGBoost, RF, and SVM—are employed to develop inversion models for estimating mangrove AGB. The model with the highest predictive accuracy is then selected to estimate mangrove AGB in the study area. This approach not only provides an effective method for estimating mangrove biomass but also offers valuable insights into the optimal model for mangrove ecosystem protection, restoration, and rehabilitation. The findings contribute to conservation and restoration efforts by providing scientifically grounded methods for monitoring and managing these critical habitats. The application of advanced machine learning techniques in blue carbon ecosystems like mangroves demonstrates the significant potential of UAV-LiDAR data in environmental monitoring, offering a robust framework for supporting ecological restoration initiatives. From the perspective of sustainability, this study is of significant importance in the assessment of ecosystem health, land use optimization, and adaptation and mitigation of climate change. By accurately monitoring the growth conditions and biomass of mangroves, it provides crucial support for global carbon balance research. Furthermore, it supplies data for the restoration and sustainable management of mangroves in coastal areas while promoting carbon sink policies and ecological conservation decisions through the long-term monitoring of biomass and carbon storage.

2. Materials and Methods

2.1. Study Area

Xinyingwan (19°50′–19°53′ N, 109°31′–109°35′ E), located in the northwestern part of Hainan Island (Figure 1), is characterized by its unique geographic position and gentle topography. The region lies within the tropical monsoon climate zone, featuring high temperatures, high humidity, and significant maritime influences. The area experiences an average annual temperature of 23–24 °C, with approximately 135.9 rainy days and a total annual precipitation of 1417.8 mm. These climatic conditions foster a diverse range of habitats that support the growth of mangrove forests and various wildlife species. Xinyingwan, situated within the study area, is renowned for its rich ecosystem and diverse species. The bay hosts several mangrove communities, as well as mixed communities comprising species such as *Rhizophora stylosa*, *Bruguiera gymnorrhiza*, *Aegiceras corniculatum*, and *Aricennia marina*. The study focuses on the mangrove wetland ecosystem along the peripheral coast of the bay, serving as a crucial area for the ecological protection and restoration of mangrove coastal wetlands in Xinyingwan. These mangrove communities play a crucial role in region biodiversity conservation and wetland restoration efforts.

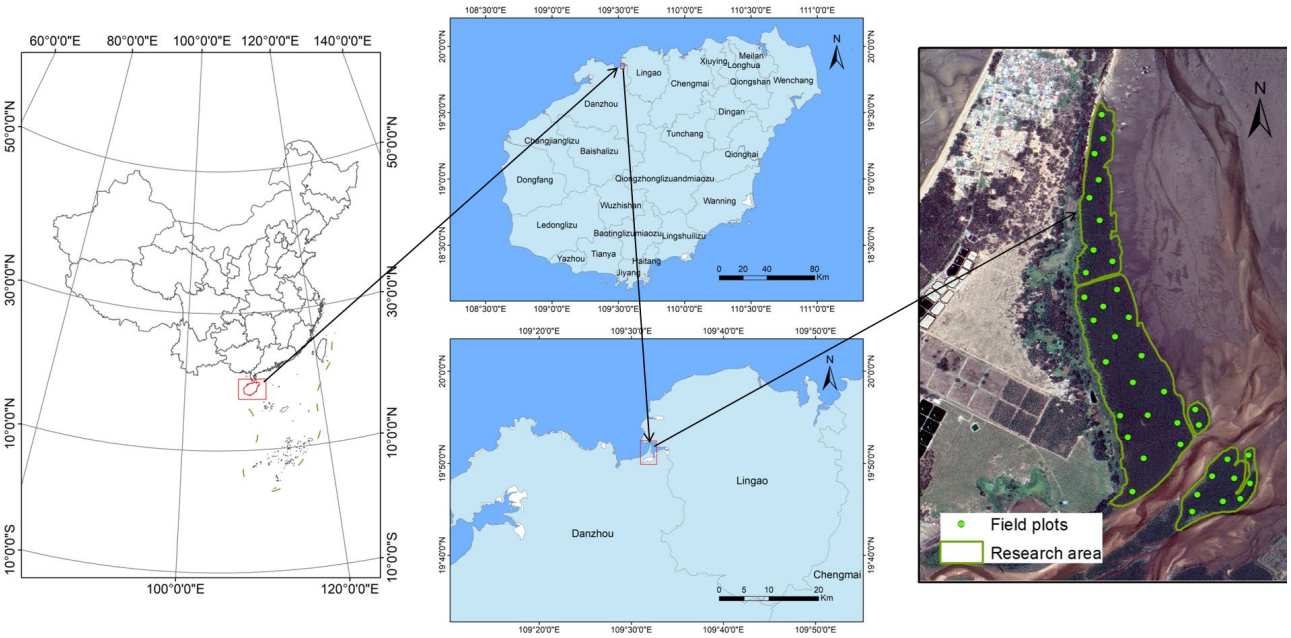


Figure 1. Location map of the research area.

2.2. Data Acquisition and Processing

2.2.1. Field Data Acquisition and Processing

In this study, a field survey of mangrove forests in the Xinyingwan area was conducted on 1–2 August 2023 during the low-tide period. The mangrove forests were primarily distributed along the peripheral coastline of the bay. Based on vegetation types, topographic features, and geomorphological characteristics, 37 sample plots, each measuring 20 m × 20 m, were established in areas exhibiting favorable vegetation growth. The main parameters measured included mangrove species, plant height, diameter at breast height (DBH), and other growth indicators. For DBH measurements, a standard breast height of 1.3 m above ground level was adhered to. The DBH of each mangrove tree within the sample plots was measured systematically using a measuring tape. Additionally, the coordinates of the center of each sample plot were recorded using a handheld global positioning system (GPS) device. To estimate the AGB of the mangrove forests, several anisotropic growth equations proposed by previous researchers were reviewed. After evaluating the

fitting accuracy of these equations, the one with the highest coefficient of determination (R^2) was selected for further calculations [52,53]. The chosen equation for estimating the AGB of *Rhizophora stylosa*, one of the dominant mangrove species in the area, is:

$$AGB = 0.235 \times D^{2.11} \quad (1)$$

where:

D: Diameter at breast height (in centimeters);

AGB: Aboveground biomass of *Rhizophora stylosa* (in kilograms).

2.2.2. UAV-LiDAR Data Acquisition and Processing

UAV-LiDAR technology integrates GPS, inertial navigation system (INS), and laser scanning ranging (LSR) to obtain high-precision 3D laser point cloud data. By leveraging multiple echo capabilities, UAV-LiDAR can effectively penetrate vegetation and rapidly acquire detailed point cloud data, even in complex terrain environments. This enables the collection of intricate 3D information on mangrove forest structures. In this study, a UAV-LiDAR system was deployed to survey the study area on 1–2 August 2023.

The raw laser point cloud data, acquired in LAS standard format following the point cloud solving process, was subject to preprocessing using LiDAR360 5.2 version software. This involved several steps: sample cropping, denoising, ground and non-ground point separation, and normalization. Derived from this processed data were digital surface models (DSMs), digital elevation models (DEMs), and canopy height models (CHMs). These models provided the basis for calculating forest stand parameters. The processed DSM, DEM, and CHM were used to extract 81 characteristic parameters, including height, intensity, and density variables. These parameters were calculated using a grid-based approach, and the results are summarized in Table 1.

Table 1. Statistical summary of point cloud features for forest stand AGB.

Type	Variables	Variable Description
Height Metrics	elev_per/elev_AIH01, 05, 10, 20, 25, 30, 40, 50, 60, 70, 75, 80, 90, 95, 99	Height percentile corresponding to all point clouds at 1%, 5%, 10%, 20%, 25%, 30%, 40%, 50%, 60%, 70%, 75%, 80%, 90%, 95%, and 99% quantile/cumulative height percentile
	elev _mean, elev _median, elev _max, elev _min, elev _madmedian	Mean, median, maximum, minimum and median absolute deviation of heights
	elev_stddev, elev_var, elev_cv, elev_kurtosis, elev_skewness, elev_crr.	Standard deviation, variance, coefficient of variation, kurtosis, skewness, canopy undulation rate of height
	elev_sqrt_mean_sq, elev_curt_mean_cube, elev_IQ, elev_AIH_IQ	Generalized mean of quadratic and cubic (root mean square/cubic root of height), interquartile spacing of heights, cumulative interquartile spacing of heights
Density Metrics	elev_density1, 2, 3, 4, 5, 6, 7, 8, 9,10	Ratio of total number of point clouds in each layer of the point cloud from bottom to top
Intensity Metrics	int_per01, 05, 10, 20, 25, 30, 40, 50, 60, 70, 75, 80, 90, 95, 99	Corresponding intensity percentiles at the 1%, 5%, 10%, 20%, 25%, 30%, 40%, 50%, 60%, 70%, 75%, 80%, 90%, 95%, and 99% quartiles of all point clouds
	int _mean, int _median, int _max, int_min, int _madmedian	Mean, median, maximum, minimum and median absolute deviation of intensity
	int _std, int _var, int _cv,int_kurtosis, int _skewness,	Standard deviation, variance, coefficient of variation, kurtosis, skewness for intensity
	int_IQ	Intensity quartile spacing

2.3. Research Methodology

2.3.1. Technical Routes

In this study, variable parameters extracted from field measurements and LiDAR data were subjected to two distinct feature selection methods. The selected features were then input into three different machine learning algorithms: random forest (RF), XGBoost, and support vector machine (SVM). Through model training, fitting, and prediction, we estimated the AGB of mangrove forests. By analyzing the performance of these models, we aimed to determine the most suitable feature variables for modeling and ultimately identify the algorithm with the highest inversion accuracy.

This study is divided into four main components: data acquisition, data preprocessing, feature extraction and screening, and the construction and accuracy assessment of AGB inversion models. UAV-mounted LiDAR was employed to acquire laser point cloud data, which underwent preliminary preprocessing. A field survey was conducted to collect mangrove forest data, including tree height, DBH, crown width (CW), and other key structural parameters. The LiDAR point cloud data underwent preprocessing, including denoising, filtering, and normalization, followed by the generation of the CHM through the interpolation of the DSM and DEM. Feature parameters were then extracted from the normalized point cloud data. The measured structural parameters of the mangroves were used in an allometric growth equation to estimate the actual AGB. Subsequently, feature selection methods were employed to select optimal parameters from the extracted feature variables and the measured AGB. The dataset was randomly portioned into a training set (80% of the data) and a testing set (20% of the data). Utilizing the selected features, the machine learning models were trained on the training set. The performance of each model was evaluated using the R^2 and root mean square error (RMSE), ultimately determining the best-performing model for AGB estimation.

This methodology provides an effective approach for estimating mangrove AGB using UAV-LiDAR data and machine learning techniques, offering valuable insights for mangrove ecosystem monitoring and conservation efforts.

2.3.2. Variable Selection Methods

Feature variable screening is essential for removing redundant or irrelevant features, as it simplifies the model, enhancing its generalizability, and reducing computational resource consumption.

1. Zero-Importance Feature Selection

Zero-importance feature selection assesses the importance of each feature in terms of its contribution to the model's predictions, and features with minimal or negligible impact are removed. This approach improves model accuracy and efficiency [54].

2. Zero-Importance Feature Selection Based on Mutual Information

Traditional zero-importance feature selection methods typically rely on model-based importance scores to evaluate the importance of features. However, this approach may overlook crucial aspects, such as feature redundancy and nonlinear correlations. Mutual information (MI) provides a more comprehensive measure of the relationship between two variables, capturing both linear and nonlinear dependencies. Unlike Pearson's correlation coefficient, which primarily measures linear relationships, and Spearman's rank correlation, which can identify nonlinear relationships but is less generalized, mutual information offers a more robust solution, especially for complex or nonlinear data.

Mutual information quantifies the degree of dependence between variables by evaluating their joint and marginal probability distributions. It is particularly advantageous in scenarios involving nonlinear or complex relationships as it can effectively detect redun-

dancy and interactions that may not be readily apparent when using traditional correlation measures. Thus, including mutual information in zero-importance feature selection allows for a more accurate and comprehensive feature-screening process. Mutual information between variables X and Y is calculated as follows:

$$MI(X,Y) = \sum_{x \in X} \sum_{y \in Y} P(x,y) \log\left(\frac{P(x,y)}{P(x)P(y)}\right) \quad (2)$$

where *P(x,y)* is the joint probability distribution of *X* and *Y*; *P(x)* and *P(y)* are the marginal probability distributions of X and Y; and the greater the difference between P(x,y) and P(x)P(y), the greater the dependence between the two variables and the greater the value of mutual information [55].

In this study, we employed kernel density estimation (KDE) to estimate probability distributions, as it can more smoothly handle continuous variables and avoids the boundary effects that may be introduced by binning methods. This approach calculates the density contributions of each data point xi and yi within a selected kernel function's surrounding area and utilizes a bandwidth parameter to control the smoothness of the kernel function. The formula is shown below:

$$P(\mathrm{x}) = \frac{1}{nh} \sum_{i=1}^{n} K\left(\frac{x - x_i}{h}\right) \quad (3)$$

$$P(\mathrm{y}) = \frac{1}{nh} \sum_{i=1}^{n} K\left(\frac{\mathrm{y} - y_i}{h}\right) \quad (4)$$

$$P(x,y) = \frac{1}{nh_x h_y} \sum_{i=1}^{n} K\left(\frac{x - x_i}{h_x}\right) K\left(\frac{\mathrm{y} - y_i}{h_y}\right) \quad (5)$$

In this context, *K* represents the kernel function and h denotes the bandwidth parameter, which is typically determined through cross-validation or heuristic selection [55,56].

2.3.3. Machine Learning Algorithms

Numerous studies have demonstrated that biomass prediction models developed using machine learning algorithms exhibit superior model fitting, prediction accuracy, and broader generalizability [49–51,57–59].

1. Random Forest Algorithm

Random forest (RF) is an ensemble learning algorithm widely employed for both classification and regression tasks, leveraging the construction of multiple decision trees. The algorithm operates by randomly selecting both samples and features through a bagging strategy, enhancing its robustness. During each tree's construction, RF randomly selects a subset of training samples, allowing each tree to be trained on slightly different data. Additionally, at each decision node, RF randomly selects a subset of features to consider for splitting, rather than using all available features. This introduces diversity into the model and mitigates the risk of overfitting [50,57].

2. Extreme Gradient Boosting Algorithm

Extreme gradient boosting (XGBoost) is a highly effective and efficient gradient boosting algorithm designed to improve model performance by sequentially adding weak learners, typically decision trees. In each iteration, XGBoost fits a new weak learner to the residuals of the preceding iteration, progressively refining the model's predictions. The algorithm aims to minimize a composite objective function that comprises a loss function and a regularization term. The loss function measures the discrepancy between predicted

and actual values, while the regularization term controls model complexity and prevents overfitting. XGBoost employs gradient descent to optimize this objective function and efficiently identify the optimal model parameters [49,58].

3. Support Vector Machine Algorithm

Support vector machine (SVM) is a powerful supervised machine learning algorithm widely used for classification, regression, and other pattern recognition tasks. SVM has proven effective in various applications, including function fitting, where it learns to classify training samples into distinct categories. The core concept of SVM classification lies in constructing a hyperplane in high-dimensional or infinite-dimensional space that maximizes the margin between classes. By maximizing the margin, SVM effectively separates data points from different classes, demonstrating its versatility in performing both classification and regression tasks [51,59].

2.3.4. Model Accuracy Assessment

From the processed LiDAR point cloud data, a comprehensive set of feature variables was extracted, and optimal variables for AGB estimation were selected through an importance analysis to reduce redundancy. Regression modeling of AGB was then performed by integrating the selected optimal variables with three machine learning algorithms. From the 41 sample data points, 80% were randomly selected to form the training set, while the remaining 20% constituted the test set. Model accuracy was evaluated by comparing R^2 and RMSE using the following formula:

$$R^2 = 1 - \frac{\sum_{i=1}^{N} (y_i - \hat{y}_i)^2}{\sum_{i=1}^{N} (y_i - \overline{y}_0)^2} \quad (6)$$

$$RMSE = \sqrt{\frac{1}{N} \sum_{i=0}^{N} (y_i - \hat{y}_i)^2} \quad (7)$$

where: y_i is the measured biomass value, $\hat{y}_i$ is the estimated biomass value, $\overline{y}$ is the mean measured biomass value, and n is the number of surveyed sample plots.

3. Results

3.1. Mangrove Identification Result

The field survey data on *Rhizophora stylosa* DBH, tree height, and crown spread are presented in Table 2. The measured DBH of *Rhizophora stylosa* ranged from 3.0 to 5.67 cm, with a mean of 4.43 cm. Tree height ranged from 1.8 to 6.0 m, with an average of 3.19 m. Individual plant AGB ranged from 2.39 to 7.62 kg, with a mean of 5.30 kg.

Table 2. Measured mangrove forest parameters.

Tree Species	Statistic	Plant Height (m)	Diameter at Breast Height (cm)	Single Plant AGB/(kg)
Rhizophora stylosa	Average value	3.19	4.43	5.3
	Maximum values	6	5.67	7.62
	Minimum value	1.8	3	2.39

3.2. Assessment of the Importance of Variables

1. Zero-Importance Feature Selection

Variable importance and cumulative importance were determined using the zero-importance feature selection method. When cumulative importance reached 98%, it was concluded that subsequent variables contributed negligibly to mangrove AGB prediction. Therefore, variables with a cumulative importance exceeding 98% were excluded from further analysis. As illustrated in Figures 2 and 3, a total of 26 feature variables were selected for modelling, of which 23 were height-related and 3 were intensity-related.

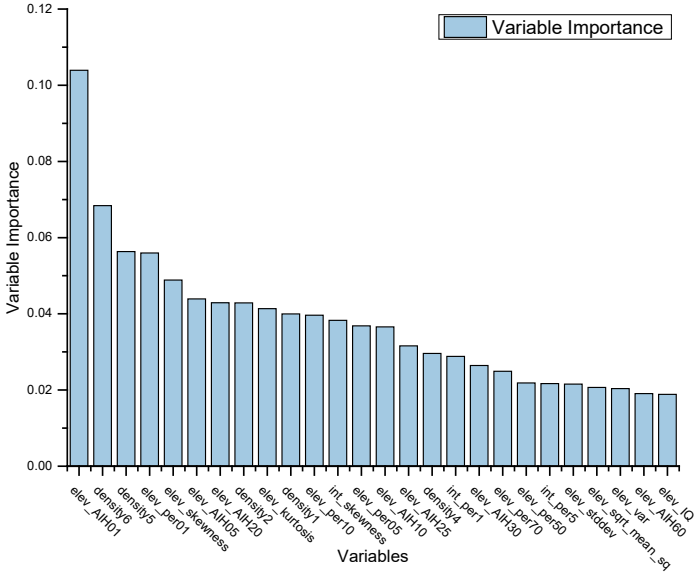


Figure 2. Ranking the importance of selected variables for mangrove forests in the study area.

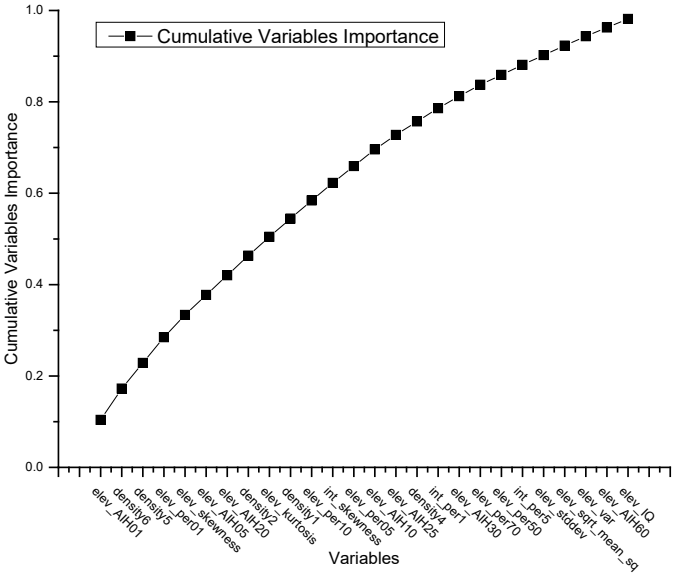


Figure 3. The cumulative importance of selected variables for mangrove forests in the study area.

2. Zero-Importance Feature Selection Based on Mutual Information

During feature screening, mutual information and feature importance scores were employed to assess, respectively, the nonlinear relationship between features and the target variable and their predictive capacity within the model. These two metrics were then combined with equal weights to generate a composite score for each feature. Specifically,

a weight of 0.5 was assigned to both mutual information and feature importance. The composite score was calculated using the following formula:

$$\text{Composite Score} = 0.5 \times \text{Mutual Information} + 0.5 \times \text{Feature Importance}$$

The features were then ranked according to their composite score, and the top 26 variables were selected for further analysis (Table 3). These selected feature variables exhibited high variance. The elev_AIH/perX metric is calculated by sorting all normalized LiDAR point cloud data within a statistical unit by height and then determining the cumulative height or height percentile. For instance, elev_AIH/per90 corresponds to the cumulative height or height percentile reached by 90% of the point cloud data. Generally, higher elev_AIH/per values indicate that the trees in the area are taller and the ecological environment is more favorable, which is often closely associated with higher AGB. The density variable represents the distribution density of point clouds at different height levels within a specific area. Density4 and density5 correspond to the proportion of echoes in the fourth and fifth height levels relative to the total number of echoes, respectively. Typically, higher "density" values may suggest denser or taller tree distributions at the corresponding height levels, reflecting a more complex forest structure and a superior growth environment in the area. The elev_skewness parameter is used to characterize the skewness of the height distribution, thereby revealing the topographic features of mangrove forests. Positive skewness indicates that the majority of the point cloud data in the area is concentrated at lower elevations, a phenomenon that often suggests mangrove growth in wet or low-lying areas where tree heights are shorter, and consequently, the AGB is lower. The 'elev_kurtosis' parameter represents the kurtosis of the height distribution, reflecting the flatness or the intensity of variation in the terrain. A higher kurtosis value indicates more pronounced variations in the terrain, which may adversely affect the stability of plant growth, potentially leading to lower AGB in mangrove forests. Conversely, a lower kurtosis value typically indicates a flatter terrain, which is conducive to stable plant growth and supports higher AGB in mangrove forests. The 'elev_sqrt_mean_sq' parameter represents the root mean square (RMS) of the terrain height in LiDAR data, revealing the roughness of the surface. A higher RMS value often indicates rough terrain, which may impact plant growth and the stability of the hydrological environment, thereby constraining mangrove growth and resulting in lower AGB. In contrast, a lower RMS value indicates a flatter terrain, which is more suitable for mangrove growth and typically promotes the formation of higher AGB.

Table 3. Comprehensive score of characteristic variables.

Variables	Overall Rating	Variables	Overall Rating	Variables	Overall Rating
elev_AIH25	0.9092	elev_per10	0.8483	elev_AIH70	0.8169
elev_AIH90	0.8983	elev_per20	0.8438	elev_AIH95	0.8100
density4	0.8935	elev_AIH40	0.8433	elev_per25	0.8038
elev_skewness	0.8836	elev_per50	0.8388	elev_AIH50	0.7992
elev_AIH30	0.8696	elev_per90	0.8289	elev_per40	0.7990
elev_AIH20	0.8681	elev_AIH60	0.8283	elev_per70	0.7953
elev_AIH10	0.8662	elev_per05	0.8278	elev_sqrt_mean_sq	0.7892
density5	0.8501	elev_per80	0.82676	elev_AIH05	0.7873
elev_per75	0.8491	elev_kurtosis	0.8182		

After filtering the feature variables using this method, the correlation between the selected feature variables was assessed using the Pearson method. The resulting correlation outcomes are illustrated in Figure 4. It can be seen from the figure that the correlation

among the selected variable groups does not exceed 0.6, indicating generally low levels of correlation.

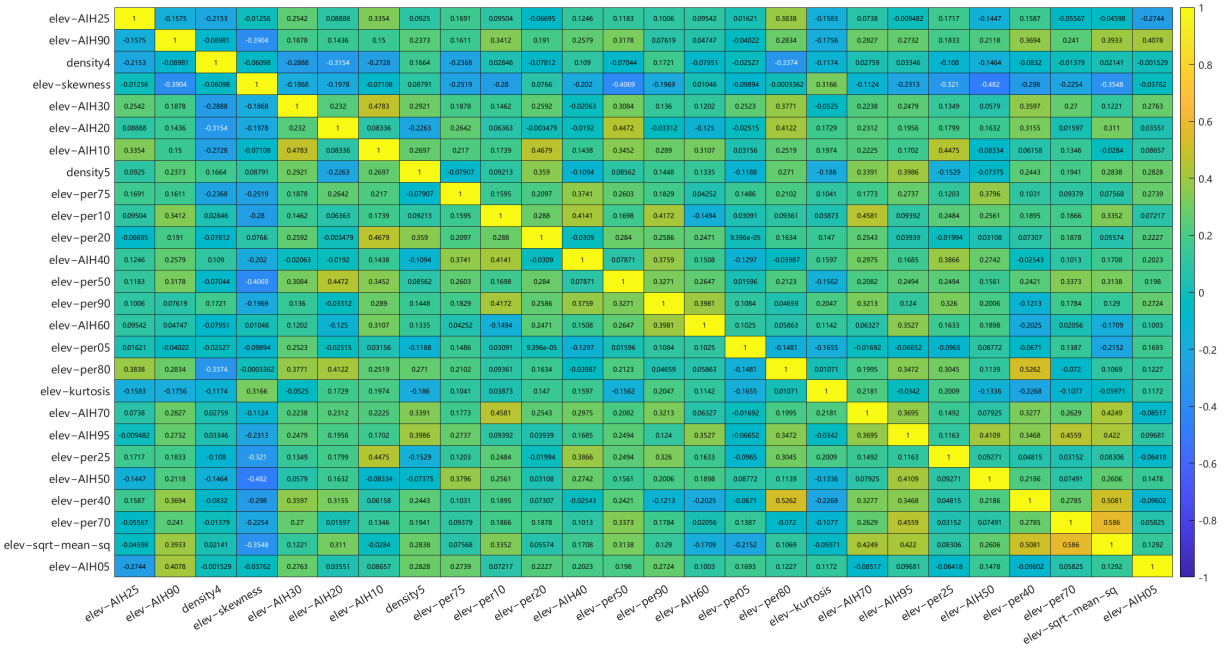


Figure 4. UAV-LiDAR point cloud parameter correlation chart.

3.3. Modeling Accuracy Evaluation and Comparison

When performing model predictions, it is generally necessary to divide the sample data into training and testing sets in order to evaluate the predictive accuracy of the forest biomass model using the testing set. Due to the limited number of samples from ground survey data and UAV-LiDAR data, this study employed Leave-One-Out Cross-Validation (LOOCV) to evaluate the model during biomass prediction. This method retains one sample as the testing set during each training iteration, while the remaining samples are used to train the model, thereby ensuring that all data can be fully utilized. However, the LOOCV method has a high computational cost, making it more suitable for situations with a small sample size.

The performance of three machine learning algorithms—SVM, RF, and XGBoost—was evaluated for estimating AGB (Figures 4 and 5). Feature variables selected through two methods—zero-importance feature selection and zero-importance feature selection based on mutual information—were input into each model. Model accuracy was assessed using R^2 and RMSE. Computational results demonstrated that, across all six comparison datasets, feature variables selected using the zero-importance feature selection method based on mutual information yielded exceptional predictive performance in the SVM model. R^2 values consistently surpassed 0.84 for both training and test sets, coupled with low RMSE values, indicating that this method effectively eliminated less influential features, resulting in a more parsimonious and interpretable model. In contrast, both the RF and XGBoost models exhibited suboptimal fitting performance, rendering them less suitable for precise mangrove AGB prediction within the study area.

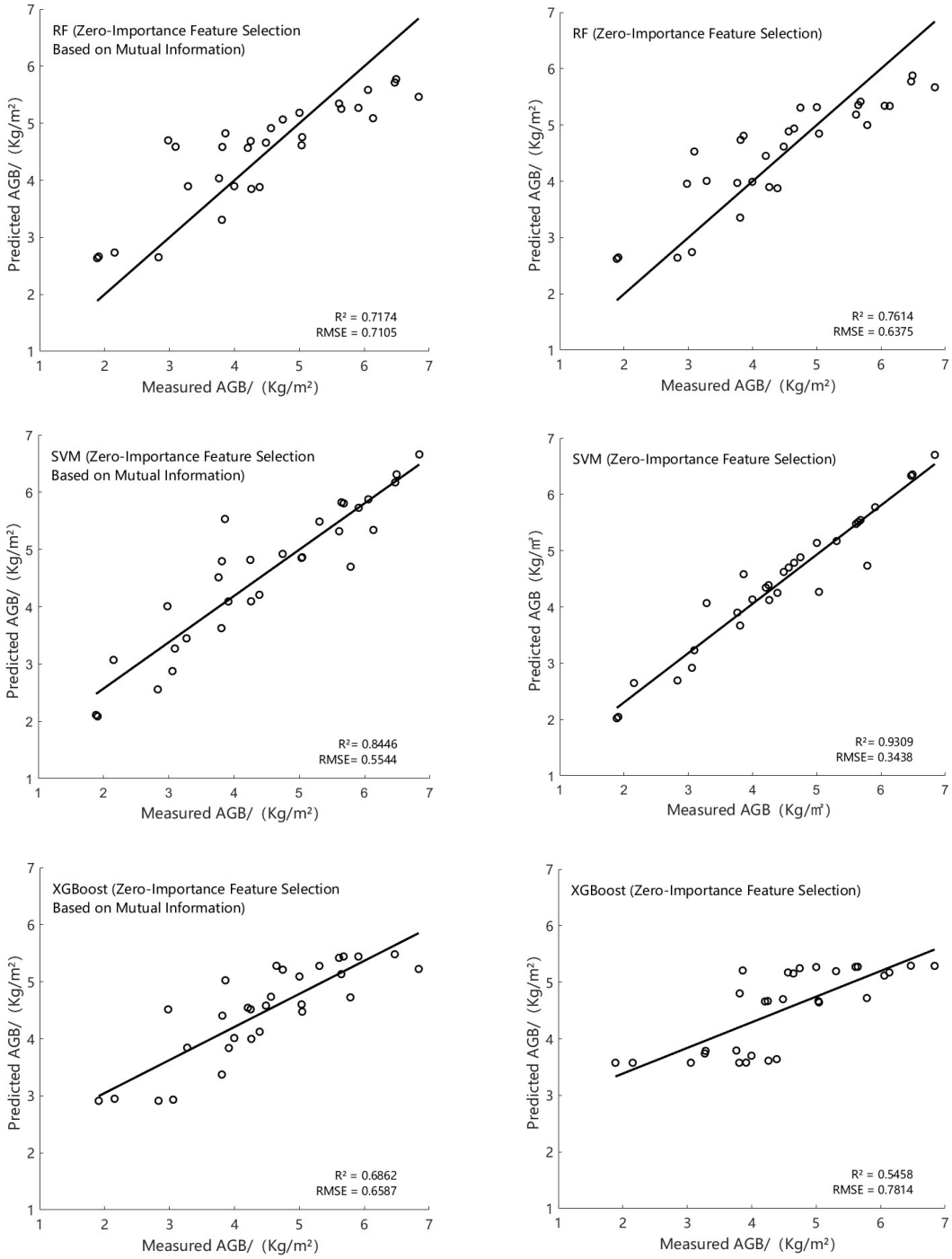


Figure 5. Scatter plots of measured AGB (X-axis) and predicted AGB (Y-axis) in two different screening methods and three different ML models (training phase).

3.4. Spatial Distribution of Mangrove Aboveground Biomass

Given the superior fitting performance of the SVM model, this study utilized the SVM model to estimate mangrove AGB across the entire study area, resulting in a mangrove AGB inversion map using ArcGIS (Figure 6). The predicted AGB values within the study area ranged from 1.97 to 5.23 kg/m^2, with a mean value of 3.83 kg/m^2, which is lower than the AGB of mangroves in Hainan Province (119.26 Mg/hm^2) [34]. The survey period and the geographical location and cultural environment of the research area can significantly influence the research results. A significant number of factors may contribute to the low biomass values observed in the mangroves of this study area, which have not been

effectively protected or restored in recent years. By observing and predicting the spatial distribution of mangrove AGB, it can be found that the AGB values of mangroves in this region are evenly distributed without much fluctuation, but the AGB of mangroves in the north and southwest are lower than those in other regions(Figure 7). The main reason may be that these two regions are close to the human activity range and have obvious traces of human habitation and production activities, while other regions are less disturbed by humans; the natural regeneration and growth process is relatively complete, the forest structure and function are relatively stable, and soil, hydrological conditions, and climate environment are relatively consistent, which provide better growth conditions for mangroves.

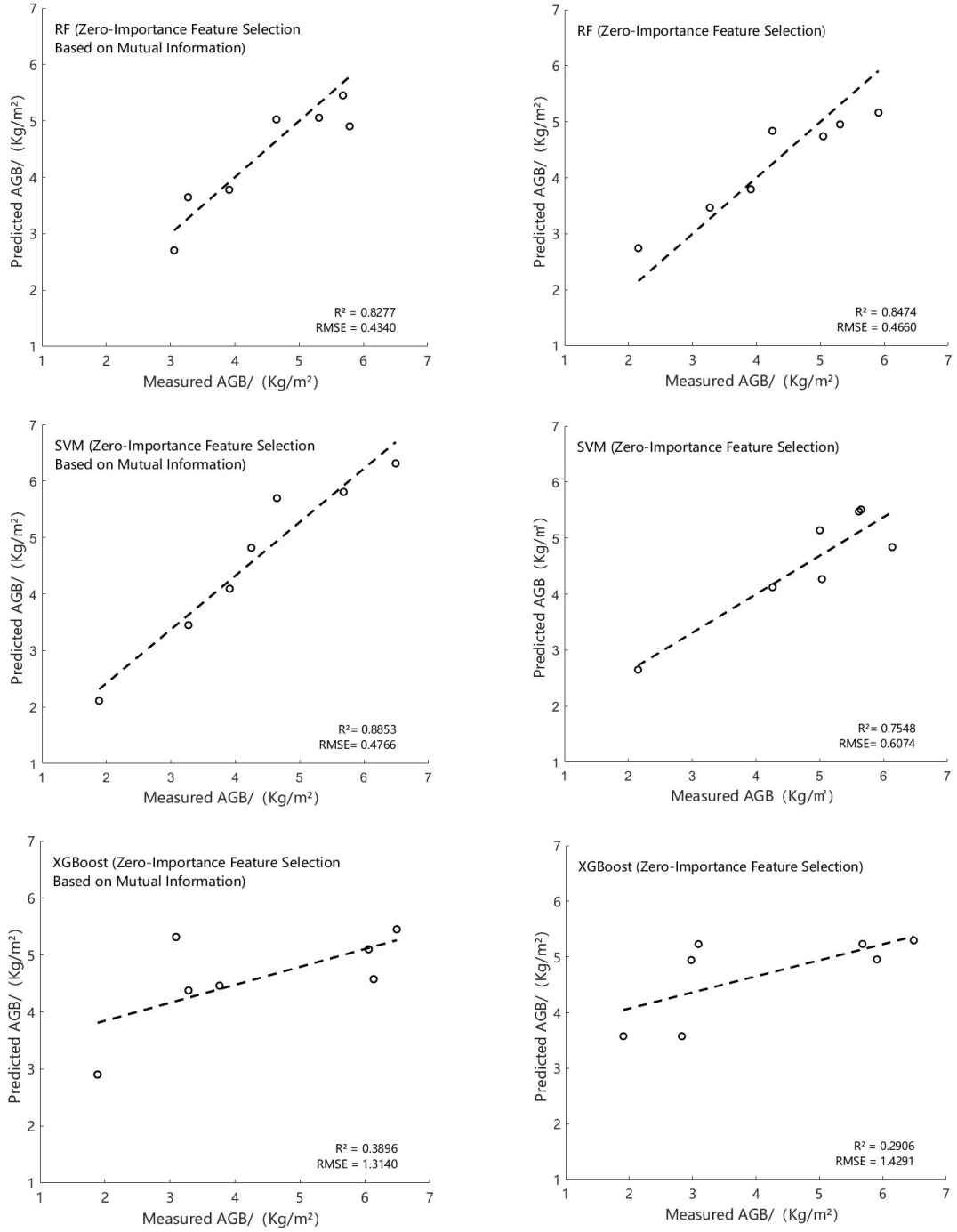


Figure 6. Scatter plots of measured AGB (X-axis) and predicted AGB (Y-axis) in two different screening methods and three different ML models (testing phase).

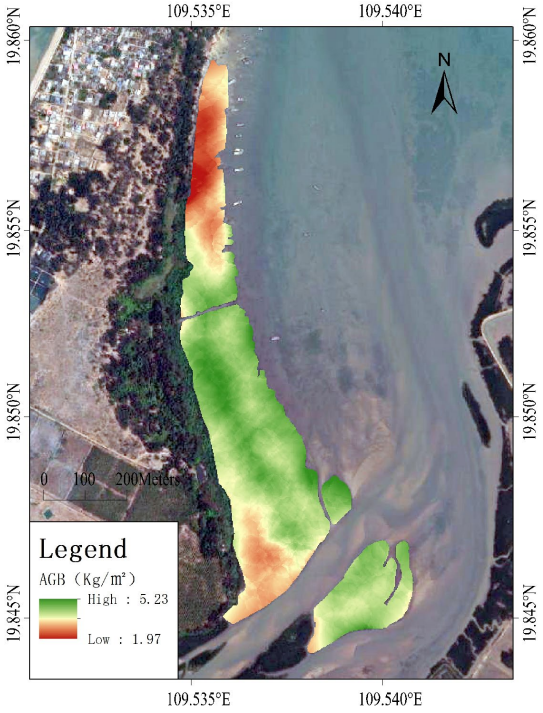


Figure 7. Spatial distribution of AGB in mangroves retrieved by SVM.

However, certain limitations inherent in the AGB estimation process were identified. UAV flight angles variability and image stitching may have adversely affected the accuracy of tree height feature extraction, consequently influencing species height estimates. Additionally, understory vegetation can obstruct the LiDAR signal, leading to errors in DEM generation and subsequent inaccuracies in tree height estimation. These factors collectively diminished the accuracy of mangrove height extraction and, consequently, AGB estimation. Future studies will be focused on investigating the impact of understory vegetation to enhance our understanding of the mangrove ecosystem and further improve the accuracy of AGB prediction.

4. Discussion

4.1. Data Selection and Variable Screening Methods

In this study, UAV-LiDAR data were chosen as the primary data source for AGB estimation due to its high spatial resolution and capacity to capture key structural features. Compared with medium-resolution optical imagery and SAR data, UAV-LiDAR significantly improves the accuracy of mangrove AGB inversion models by providing a precise three-dimensional spatial information representation.

While the recognized importance of feature selection in the machine learning-based model is widely acknowledged, limited research has comprehensively explored the application of mutual information-based zero-importance feature variable screening methods within the context of mangrove AGB estimation. In contrast to traditional feature selection approaches, this method effectively identifies variables with strong correlations to the target variable (AGB), thereby substantially enhancing model prediction accuracy. In the present study, the feature importance was evaluated using this method, and the results indicated that the most influential feature variables were primarily associated with high correlation indices. These findings underscore the distinct advantages of LiDAR data in capturing canopy structure and height variations, crucial elements for accurate AGB estimation. Furthermore, the 26 feature variables selected through this approach were

predominantly height-related, underscoring the critical role of height metrics in developing robust AGB prediction models.

4.2. Inversion Model Selection

Historically, mangrove biomass estimation has predominantly relied on linear regression models. However, linear regression imposes stringent assumptions on the data and often struggles to accurately capture complex nonlinear relationships, thereby limiting its predictive capabilities. In recent years, nonparametric models have garnered significant attention, with machine learning algorithms emerging as powerful and versatile tools for addressing these challenges. These algorithms excel at identifying intricate patterns and effectively handling nonlinear relationships, making them highly suitable for ecological modeling applications. Among various machine learning techniques, SVM stands out due to their robust nonlinear fitting capabilities. SVM can effectively address complex boundary problems and exhibit remarkable resilience to noise and overfitting, which are prevalent issues in ecological datasets. As a result, SVM has become an essential tool for estimating mangrove biomass [51,58]. RF, another powerful algorithm, is particularly adept at handling high-dimensional feature spaces and complex data structures. Their inherent feature selection process helps to reduce model variance and mitigate the risk of overfitting, making them particularly effective in the presence of noisy data and missing values. These strengths position RF as a key method in mangrove AGB estimation [50,57]. XGBoost, known for its rapid training speed and strong predictive performance, refines model accuracy iteratively by addressing previous model deficiencies. Moreover, XGBoost offers excellent interpretability and flexibility, making it highly adaptable for diverse data types and a preferred choice in mangrove biomass estimation [49,58]. To this end, we selected three machine learning algorithms—SVM, RF, and XGBoost—to estimate the AGB of mangrove forests in Xinyingwan. Our results demonstrate that SVM excels in handling high-dimensional feature spaces and extracting meaningful insights from complex datasets. After model tuning and validation, the final SVM model achieved an R^2 value exceeding 0.84 for both training and test sets, with a low root mean square error. These findings further validate the efficacy of the selected feature variables and the SVM model in accurately estimating mangrove AGB.

4.3. Research Deficiencies and Future Research Directions

(1) The zero-importance feature selection method based on mutual information has certain advantages in feature selection, but it also has some drawbacks and limitations. This method relies on accurate estimation of mutual information, which is sensitive to data distribution and sample size. Particularly in high-dimensional data or small sample scenarios, this can lead to inaccurate estimations, thereby affecting the reliability of feature selection. Furthermore, the method has a high computational complexity, especially when handling large-scale data, as the time and space costs of computing mutual information are substantial, which restricts its scalability in practical applications.

Future research can improve the estimation methods of mutual information, particularly focusing on robustness in high-dimensional data and small sample sizes. This can be achieved by integrating other feature selection methods, such as model-based feature importance or embedded methods, to compensate for the shortcomings of the mutual information approach, thereby forming a feature selection framework that combines multiple methods. Finally, for large-scale data, efficient algorithms and parallel computing techniques can be explored to reduce computational complexity and enhance the practical applicability of the methods.

(2) Current UAV-LiDAR-based AGB inversion studies are predominantly region-specific, with models optimized for particular areas. These models may not maintain comparable accuracy when applied to different regions due to variations in mangrove growth conditions, such as climate, soil properties, and nutrient availability, leading to potential declines in estimation precision during cross-regional applications.

Future research should focus on addressing the complex topography, extensive root distribution, and limited applicability of existing models within mangrove ecosystems. This is essential to enhance the accuracy of surface point extraction, the precision of canopy height calculations, and the universality of AGB inversion models.

5. Conclusions

This study employed UAV-LiDAR to acquire high-resolution laser point cloud data in the hi-tech Xinyingwan region of Hainan. Extracted laser point cloud data, along with measured mangrove AGB values, were input into three machine learning models to assess and compare their fitting performance. The primary objective was to identify the most accurate model for estimating mangrove AGB in the study area. The main conclusions are as follows:

(1) The SVM model exhibited the highest fitting ability for mangrove AGB estimation; with the addition of a zero-importance feature selection method based on mutual information, the test set accuracy reached an R^2 of 0.8853 and RMSE of 0.4766 kg/m^2, while the test set accuracy was R^2 of 0.7548 and RMSE of 0.6074 kg/m^2 when combined with the zero-importance feature variable selection method. Application of the mutual information-based zero-importance feature selection method to the RF and XGBoost models resulted in less impressive test set accuracies. RF achieved R^2 = 0.8277 and RMSE = 0.4340 kg/m^2, while XGBoost resulted in R^2 = 0.3896 and RMSE = 1.3140 kg/m^2. Compared with SVM, the fitting capability is relatively less prominent, and the prediction accuracy indicates that XGBoost is less suitable for estimating mangrove AGB in this region. These results underscore the effectiveness of the mutual information-based zero-importance feature selection method in identifying key variables and highlight the superior performance of the SVM model for mangrove AGB estimation. This study substantially enhances accuracy of mangrove AGB inversion and provides innovative methods for future research.

(2) Predicted AGB values for mangrove forests in the study area ranged from a low value of 1.97 kg/m^2 to a high value of 5.23 kg/m^2, with an average value of 3.83 kg/m^2. This distribution reflects relatively uniform growth conditions in the study area, primarily due to the pristine state of the mangrove ecosystem and minimal human disturbance.

(3) Canopy height, a key LiDAR-derived feature, played a critical part in improving the accuracy of mangrove AGB estimation. The inclusion of canopy height features in the model remarkably enhanced predictive capability compared with intensity features, also derived from LiDAR data. These results highlight the importance of vertical structure in accurately modeling AGB in mangrove ecosystems.

(4) The estimation of aboveground biomass in mangrove forests provides crucial references for the protection and restoration of mangrove ecosystems in the region, contributing to the sustainable development of the local ecosystem.

Author Contributions: Conceptualization, methodology, software, formal analysis, data curation, writing—original draft preparation, S.H.; validation, Z.Z. and Y.S.; investigation, Y.S., S.H., W.S. and J.M.; writing—review and editing, Z.Z. and Y.S.; supervision, Z.Z. and Y.S. All authors have read and agreed to the published version of the manuscript.

Funding: This research received no external funding.

Institutional Review Board Statement: Not applicable.

Informed Consent Statement: Not applicable.

Data Availability Statement: Data are contained within the article.

Acknowledgments: We would like to express our sincere gratitude to everyone who worked on the field survey.

Conflicts of Interest: The authors declare no conflicts of interest.

References

1. Zhu, K.; Liao, B.; Zhang, J. Studies on the Biomass of Mangrove Plantation of *Sonneratia apetala* and Bruguiera gymnorrhiza in the Wetland of Nansha in Guangzhou City. *For. Res.* **2011**, *24*, 531–536.
2. Murdiyarso, D.; Purbopuspito, J.; Kauffman, J.B.; Warren, M.W. The potential of Indonesian mangrove forests for global climate change mitigation. *Nat. Clim. Change* **2015**, *5*, 1089–1092. [CrossRef]
3. He, B.; Fan, H.; Wang, M.; Lai, T.; Wang, W. Species diversity in mangrove wetlands of China and its causation analyses. *Acta Ecol. Sin.* **2007**, *27*, 4859–4870.
4. Sheng, N.; Xin, K.; Liao, B. Literature Analysis Concerning Studies of Ecological Functions and Values of Mangrove Wetland. *Wetl. Sci. Manag.* **2021**, *17*, 47–50.
5. Dech, S.; Gebhardt, S.; Kuenzer, C.; Vo, T.Q.; Bluemel, A. Remote Sensing of Mangrove Ecosystems: A Review. *Remote Sens.* **2011**, *3*, 878–928. [CrossRef]
6. Wang, F.; Tang, J.; Ye, S.; Liu, J. Blue Carbon Sink Function of Chinese Coastal Wetlands and Carbon Neutrality Strategy. *Bull. Chin. Acad. Sci.* **2021**, *36*, 241–251.
7. Zhou, C.; Mao, T.; Xu, X.; Fang, C.; Luo, Y.; Li, B. Preliminary Analysis of C Sequestration Potential of Blue Carbon Ecosystems on Chinese Coastal Zone. *Sci. Sin. (Vitae)* **2016**, *46*, 475–486.
8. Duarte, C.M.; Middelburg, J.J.; Caraco, N. Major role of marine vegetation on the oceanic carbon cycle. *Biogeosciences* **2005**, *2*, 1–8. [CrossRef]
9. Mcleod, E.; Chmura, G.L.; Bouillon, S.; Salm, R. A blueprint for blue carbon: Toward an improved understanding of the role of vegetated coastal habitats in sequestering CO_2. *Front. Ecol. Environ.* **2011**, *9*, 552–560. [CrossRef]
10. Wang, F.; Sanders, C.J.; Santos, I.R.; Tang, J. Global blue carbon accumulation in tidal wetlands increases with climate change. *Natl. Sci. Rev.* **2021**, *8*, nwaa296. [CrossRef]
11. Bouillon, S.; Borges, A.V.; Castañeda-Moya, E.; Diele, K.; Dittmar, T.; Duke, N.C.; Kristensen, E.; Lee, S.Y.; Marchand, C.; Middelburg, J.J.; et al. Mangrove production and carbon sinks: A revision of global budget estimates. *Glob. Biogeochem. Cycles* **2008**, *22*, GB2013. [CrossRef]
12. Leal, M.; Spalding, M.D. *The State of the World's Mangroves 2022*; Global Mangrove Alliance: Washington, DC, USA, 2022.
13. Goldberg, L.; Lagomasino, D.; Thomas, N.; Fatoyinbo, T. Global declines in human-driven mangrove loss. *Glob. Change Biol.* **2020**, *26*, 5844–5855. [CrossRef]
14. Polidoro, B.A.; Carpenter, K.E.; Collins, L.; Duke, N.C.; Ellison, A.M.; Ellison, J.C.; Farnsworth, E.J.; Fernando, E.S.; Kathiresan, K.; Koedam, N.E.; et al. The loss of species: Mangrove extinction risk and geographic areas of global concern. *PLoS ONE* **2010**, *5*, e10095. [CrossRef]
15. Food and Agriculture Organization of the United Nations (FAO). *The World's Mangroves 2000–2020*; FAO: Rome, Italy, 2023. [CrossRef]
16. Zhao, N. "Ocean Guardian" Contributes to Carbon Neutrality. *China Natural Resources News*, 30 September 2021; p. 005.
17. Hu, A. China's Goal of Achieving Carbon Peak by 2030 and Its Main Approaches. *J. Beijing Univ. Technol. (Soc. Sci. Ed.)* **2021**, *21*, 1–15.
18. Tan, Y.; Tian, Y.; Huang, Z.; Zhang, Q.; Tao, J.; Liu, H.; Yang, Y.; Zhang, Y.; Lin, J.; Deng, J. Aboveground biomass of *Sonneratia apetala* mangroves in Mawei Sea of Beibu Gulf based on XGBoost machine learning algorithm. *Acta Ecol. Sin.* **2023**, *43*, 4674–4688.
19. Zhang, S. Application of UAV in Inversion of Aboveground Biomass and Carbon Storage of Dense Low Shrub Mangrove. Ph.D. Thesis, Guangxi University, Nanning, China, 2022.
20. Zhao, T.; Yu, R.; Zhang, Z.; Bai, X.; Zeng, Q. Estimation of wetland vegetation aboveground biomass based on remote sensing data: A review. *Chin. J. Ecol.* **2016**, *35*, 1936–1946.
21. Xu, F. Mangrove Extraction and Carbon Storage Estimation by Using Sentinel-2 Images. Ph.D. Thesis, Lanzhou Jiaotong University, Lanzhou, China, 2020.
22. Zheng, D.; Rademacher, J.; Chen, J.; Crow, T.; Bresee, M.; Moine, J.L.; Ryu, R.S. Estimating aboveground biomass using Landsat 7 ETM+ data across a managed landscape in northern Wisconsin, USA. *Remote Sens. Environ.* **2004**, *93*, 402–411. [CrossRef]

23. Cornejo, R.H.; Koedam, N.; Luna, A.R.; Troell, M.; Dahdouh-Guebas, F. Remote Sensing and Ethnobotanical Assessment of the Mangrove Forest Changes in the Navachiste-San Ignacio-Macapule Lagoon Complex, Sinaloa, Mexico. *Ecol. Soc.* **2005**, *10*, 16. [CrossRef]
24. Hall, R.J.; Skakun, R.S.; Arsenault, E.J.; Case, B.S. Modeling forest stand structure attributes using Landsat ETM+ data: Application to mapping of aboveground biomass and stand volume. *For. Ecol. Manag.* **2006**, *225*, 378–390. [CrossRef]
25. Cao, Q.; Xu, D.; Ju, H. Biomass Estimation of Five Kinds of Mangrove Community with the KNN Method Based on the Spectral Information and Textural Features of TM Images. *For. Res.* **2011**, *24*, 144–150.
26. Hirata, Y.; Tabuchi, R.; Patanaponpaiboon, P.; Poungparn, S.; Yoneda, R.; Fujioka, Y. Estimation of aboveground biomass in mangrove forests using high-resolution satellite data. *J. For. Res.* **2014**, *19*, 34–41. [CrossRef]
27. Pham, L.T.H.; Brabyn, L. Monitoring mangrove biomass change in Vietnam using SPOT images and an object-based approach combined with machine learning algorithms. *ISPRS-J. Photogramm. Remote Sens.* **2017**, *128*, 86–97. [CrossRef]
28. Li, Q.; Xuan, C.; Tang, Z.; Zhang, T.; Song, Y.A. Review on Vegetation Biomass Inversion Based on Remote Sensing Technology. *J. Inn. Mong. Agric. Univ. (Nat. Sci. Ed.)* **2024**, 1–13.
29. Li, W.; Xue, Z.; Zhu, J.; Tian, Z. Estimation of carbon stock of the mangrove forests in Hainan Island based on multi-source remote sensing data from GEE platform. *Remote Sens. Nat. Resour.* **2024**, 1–8.
30. Zhang, S.; Hui, G.; Han, Z.; Sun, S.; Tian, X. Estimation of Large-scale Forest Above-ground Biomass based on Fast Optimizing Remotely Sensed Features from Pptical Multi-spectral and SAR Data. *Remote Sens. Technol. Appl.* **2019**, *34*, 925–938.
31. Lucas, R.; Rebelo, L.M.; Fatoyinbo, L.; Rosenqvist, A.; Itoh, T.; Shimada, M.; Simard, M.; Souza-Filho, P.W.; Thomas, N.; Trettin, C.; et al. Contribution of L-band SAR to systematic global mangrove monitoring. *Mar. Freshw. Res.* **2014**, *65*, 589–603. [CrossRef]
32. Bai, M.; Zhang, C.; Chen, Q.; Wang, J.; Li, H.; Shi, X.; Tian, X.; Zhang, Y. Study on the Extraction of Individual Tree Height Based on UAV Visual Spectrum Remote Sensing. *For. Grassl. Resour. Res.* **2021**, 164–172.
33. Li, X.; Wu, J.; Lin, W. Forest biomass estimation and mapping based on high resolution UAV images. *J. Cent. S. Univ. For. Technol.* **2020**, *40*, 50–56.
34. Wang, D.; Wan, B.; Liu, J.; Su, Y.; Guo, Q.; Qiu, P.; Wu, X. Estimating aboveground biomass of the mangrove forests on northeast Hainan Island in China using an upscaling method from field plots, UAV-LiDAR data and Sentinel-2 imagery. *Int. J. Appl. Earth Obs. Geoinf.* **2020**, *85*, 101986. [CrossRef]
35. Yu, C.; Gong, H.; Cao, J.; Liu, Y.; Liu, K. Individual Tree Crown Delineation and Aboveground Biomass Estimation of *Sonneratia apetala* Based on Unmanned Aerial Vehicle Remote Sensing Images. *Trop. Geogr.* **2023**, *43*, 12–22.
36. Wu, P.; Ren, G.; Zhang, C.; Wang, H.; Liu, S.; Ma, Y. Fine identification and biomass estimation of mangroves based on UAV multispectral and LiDAR. *Natl. Remote Sens. Bull.* **2022**, *26*, 1169–1181. [CrossRef]
37. Salum, R.B.; Robinson, S.A.; Rogers, K. A Validated and accurate method for quantifying and extrapolating mangrove aboveground biomass using LiDAR data. *Remote Sens.* **2021**, *13*, 2763. [CrossRef]
38. Pereira, F.R.D.S.; Kampel, M.; Soares, M.L.G.; Estrada, G.C.D.; Bentz, C.; Vincent, G. Reducing uncertainty in mapping of mangrove aboveground biomass using airborne discrete return lidar data. *Remote Sens.* **2018**, *10*, 637. [CrossRef]
39. Jia, Y.; Zhang, L.; Wu, D.; Song, C.; Yuan, W.; Li, L. Comparative analysis of grassland biomass inversion models based on unmanned aerial vehicle multispectral data. *Acta Ecol. Sin.* **2024**, *44*, 1–11.
40. Luo, J.; Tian, Y.; Zhang, Q.; Tao, J.; Huang, Y.; Wang, J.; Zhang, Y.; Huang, Z.; Deng, J.; Tan, Y. Estimation of aboveground biomass of mangrove forest using UAV-LiDAR. *Haiyang Xuebao* **2023**, *45*, 108–119.
41. Li, X.; Liu, X.; Sun, B.; Jiang, J.; Yu, H.; Wu, D.; Du, X.; Wang, H.; Jia, J.; Yang, H. Machine learning–based assessment of grassland aboveground biomass in Gansu Province. *Pratacultural Sci.* **2024**, *41*, 297–307.
42. Mu, Z.; Zhang, Z.; Zhang, H.; Jiang, L. Applying Machine Learning Algorithm Models to Predict Aboveground Biomass of *Larix gmelinii* in Xing'an. *J. Northeast. For. Univ.* **2024**, *52*, 41–47.
43. Wang, X.; Yang, X.; Zhao, F.; An, B.; Huang, X. Estimation of Aboveground Biomass in the Arid Oasis Based on the Machine Learning Algorithm. *Ecol. Environ. Sci.* **2023**, *32*, 1007–1015.
44. Yang, Y.; Yang, D.; Sun, H.; Meng, H.; Tian, C.; Liu, C.; Lei, D. Estimation of cotton biomass in southern Xinjiang based on UAV multi-spectral remote sensing and machine learning algorithm. *Jiangsu Agric. Sci.* **2023**, *51*, 179–187.
45. Zhang, Z.; Tian, Y.; Deng, J.; Yao, G.; Li, Y. Biomass inversion of typical mangrove forests in Qinzhou Bay based on LiDAR. *Ecol. Sci.* **2024**, *43*, 203–210.
46. Zhang, P.; Ma, Q.; Lu, J.; Ji, J.; Li, Z. Application of machine learning algorithms in estimation of above-ground biomass of forest. *Bull. Surv. Mapp.* **2021**, 28–32.
47. Tian, Y.; Huang, H.; Zhou, G.; Zhang, Q.; Tao, J.; Zhang, Y.; Lin, J. Aboveground mangrove biomass estimation in Beibu Gulf using machine learning and UAV remote sensing. *Sci. Total Environ.* **2021**, *781*, 146816. [CrossRef]
48. Jozdani, S.E.; Johnson, B.A.; Chen, D. Comparing Deep Neural Networks, Ensemble Classifiers, and Support Vector Machine Algorithms for Object-Based Urban Land Use/Land Cover Classification. *Remote Sens.* **2019**, *11*, 1713. [CrossRef]

49. Hakkal, S.; Lahcen, A.A. XGBoost To Enhance Learner Performance Prediction. *Comput. Educ. Artif. Intell.* **2024**, *7*, 100254. [CrossRef]
50. Wu, Z.; Yao, F.; Zhang, J.; Liu, H. Estimating Forest Aboveground Biomass Using a Combination of Geographical Random Forest and Empirical Bayesian Kriging Models. *Remote Sens.* **2024**, *16*, 1859. [CrossRef]
51. Deb, D.; Deb, S.; Chakraborty, D.; Singh, J.P.; Singh, A.K.; Dutta, P.; Choudhury, A. Aboveground biomass estimation of an agro-pastoral ecology in semi-arid Bundelkhand region of India from Landsat data: A comparison of support vector machine and traditional regression models. *Geocarto Int.* **2020**, *37*, 1043–1058. [CrossRef]
52. Tamai, S.; Lampa, P. Establishment and growth of mangrove seedling in mangrove forests of southern Thailand. *Ecol. Res.* **1988**, *3*, 227–238. [CrossRef]
53. Fromard, F.; Puig, H.; Mougin, E.; Marty, G.; Betoulle, J.L.; Cadamuro, L. Structure, above-ground biomass and dynamics of mangrove ecosystems: New data from French Guiana. *Oecologia* **1998**, *115*, 39–53. [CrossRef]
54. Li, N.; Wang, Y.; Zhou, L.; Zou, C.; Tian, Y.; Guo, N. DDoS Attack Random Forest Detection Method Based on Secondary Screening of Feature Importance. *Comput. Sci.* **2021**, *48* (Suppl. S1), 464–467+476.
55. Lv, X.; Li, Q.; Zhang, D.; Zeng, L.; Ling, L. Novel optimal sub-models selection algorithm for combination orecasting based on neighborhood mutual information. *Comput. Eng. Des.* **2024**, *45*, 1359–1367.
56. Zhang, Q.; Liu, S.; Wang, J.; Li, Z.; Wen, C. Feature selection for multi-labeled data based on label enhancement technique and mutual information. *Inf. Sci.* **2024**, *679*, 121113. [CrossRef]
57. Zhang, P.; Liang, Y.; Liu, B.; Ma, T.; Wu, M. Remote sensing estimation of forest aboveground biomass in Tibetan Plateau based on random forest model. *Chin. J. Ecol.* **2023**, *42*, 415–424.
58. Jia, Z.; Zhang, Z.; Cheng, Y.; Buhebaoyin; Borjiginet, S.; Quan, Z. Grassland biomass spatiotemporal patterns and response to climate change in eastern Inner Mongolia based on XGBoost model estimates. *Ecol. Indic.* **2024**, *158*, 111554. [CrossRef]
59. Shang, K. The Study of Grassland Above Ground Biomass Inversion based on Support Vector Machine Regression. Ph.D. Thesis, Southwest Forestry University, Kunming, China, 2015.

Disclaimer/Publisher's Note: The statements, opinions and data contained in all publications are solely those of the individual author(s) and contributor(s) and not of MDPI and/or the editor(s). MDPI and/or the editor(s) disclaim responsibility for any injury to people or property resulting from any ideas, methods, instructions or products referred to in the content.